JVI Journals.ASM.org

Crystal Structure of the Nipah Virus Phosphoprotein Tetramerization Domain

Jessica F. Bruhn,[a] Katherine C. Barnett,[a]* Jaclyn Bibby,[b] Jens M. H. Thomas,[c] Ronan M. Keegan,[d] Daniel J. Rigden,[c] Zachary A. Bornholdt,[a] Erica Ollmann Saphire[a,e]

Department of Immunology and Microbial Science, The Scripps Research Institute, La Jolla, California, USA[a]; Department of Chemistry, Robert Robinson Laboratories, University of Liverpool, Liverpool, United Kingdom[b]; Institute of Integrative Biology, University of Liverpool, Liverpool, United Kingdom[c]; RCaH, STFC Rutherford Appleton Laboratory, Chilton, United Kingdom[d]; The Skaggs Institute for Chemical Biology, The Scripps Research Institute, La Jolla, California, USA[e]

The Nipah virus phosphoprotein (P) is multimeric and tethers the viral polymerase to the nucleocapsid. We present the crystal structure of the multimerization domain of Nipah virus P: a long, parallel, tetrameric, coiled coil with a small, α-helical cap structure. Across the paramyxoviruses, these domains share little sequence identity yet are similar in length and structural organization, suggesting a common requirement for scaffolding or spatial organization of the functions of P in the virus life cycle.

Nipah virus is a newly emergent, bat-borne paramyxovirus found in Southeast Asia that causes encephalitis in humans with 40 to 90% lethality (1, 2). There are no vaccines or antiviral therapeutics approved for human use (3). Nipah virus has a single-stranded, negative-sense RNA genome that is encapsidated by the nucleoprotein (N) (1) and transcribed and replicated by the polymerase protein (L) (4). The phosphoprotein (P) plays an essential role as a polymerase cofactor, enhancing polymerase processivity and allowing the encapsidation of the newly synthesized viral genomes and antigenomes (4). In these roles, P serves as a tether between the polymerase and its template and also serves as a chaperone for nascent, RNA-free N, termed N^0, preventing it from nonspecifically binding host RNA (5). P has an additional role in immunosuppression: blocking interferon signaling by binding host STAT-1 (6, 7).

The N-terminal domain (NTD; residues 1 to 469) of Nipah virus P is intrinsically disordered and contains the binding site for N^0 (residues 1 to 50) (5, 8–10). The C-terminal region of P contains a well-ordered P multimerization domain (PMD; residues 470 to 578), a flexible linker, and the X domain (XD; residues 660 to 709), which mediates binding to the nucleocapsid (5, 8–10). Multimerization of the P protein is critical for genome replication (11, 12). Crystal structures of the multimerization domains of P from the paramyxoviruses Sendai virus, measles virus, and mumps virus have been determined (13–15). All three structures are composed of long, tetrameric coiled coils. Notably, the mumps virus structure is antiparallel (14) while the Sendai virus and measles virus structures are parallel (13, 15). There is minimal sequence identity in this domain among these paramyxoviruses (5 to 26%) (16, 17), and no high-resolution structure has yet been described for this key domain of Nipah virus. Blocquel et al. have recently proposed that this domain of Nipah virus forms a trimeric coiled coil, in contrast to the tetrameric coiled coils of the other paramyxoviruses (18). Their findings are based on biophysical data, including analytical ultracentrifugation, chemical cross-linking, and small-angle X-ray scattering (SAXS) (18).

In order to provide a high-resolution experimental structure, the multimerization domain of Nipah virus P (residues 470 to 578) was cloned into pET46 and expressed in *Escherichia coli* with an N-terminal 6×His tag followed by a tobacco etch virus (TEV) protease cleavage site. The protein was purified via nickel affinity, ion-exchange (MonoQ), and size exclusion chromatography coupled to multiangle light scattering/refractive index (SEC/MALS). The protein elutes from SEC/MALS with an apparent molecular mass of 52.5 kDa, suggesting that it is a tetramer in solution (57.2 kDa is expected for a tetramer, and 42.9 kDa is expected for a trimer). After TEV removal of the 6×His tag, the protein was crystallized in 0.1 M imidazole (pH 7.0), 25% polyethylene glycol MME 550 and cryoprotected in mother liquor diluted with 15% glycerol. Data to 2.2 Å were collected at Advanced Light Source (ALS; Berkeley, CA) beamline 5.0.2 and processed by using HKL3000 and d*TREK (19, 20). The crystal used for structure determination belongs to space group P1 (Table 1). Other crystals, which diffracted to somewhat lower resolution, belong to space groups I422, $P42_12$, and C2 (Table 1). All crystal forms showed strong off-origin peaks in self-Patterson maps with a distance of 5.15 Å from the origin (22, 23). These peaks correspond to the length of one full turn of an α-helix and result from intrahelical vectors of long helices all oriented in the same direction (24) and are strongly suggestive of an inherent coiled-coil structure (25).

The multimerization domains of the Sendai virus (15), measles virus (13), and mumps virus (14) P proteins failed to generate successful molecular replacement solutions. This Nipah virus structure was eventually determined by using the automated pipeline AMPLE (26), which performs molecular replacement searches using ab initio models. Here, AMPLE was used differently: to cluster and truncate a set of 100 comparative models for Nipah virus P that were generated by ROSETTA (27), using

Received 15 August 2013 **Accepted** 16 October 2013
Published ahead of print 23 October 2013
Address correspondence to Erica Ollmann Saphire, erica@scripps.edu.
* Present address: Katherine Barnett, Program in Virology, Harvard University, Boston, Massachusetts, USA.
This is report 25023 from The Scripps Research Institute.

doi:10.1128/JVI.02294-13

TABLE 1 Data collection and refinement statistics for the multimerization domain of Nipah virus P

Parameter	Value(s) for space group:			
	P1	I422	$P42_12$[e]	C2[f]
Beamline	ALS 5.0.2	ALS 5.0.2	ALS 5.0.3	ALS 5.0.2
Wavelength (Å)	1.0000	1.0000	0.976548	1.0000
Cell dimensions				
a, *b*, *c* (Å)	48.06, 76.88, 80.75	44.67, 44.67, 275.23	96.09, 96.09, 127.96	142.89, 55.64, 77.84
α, β, γ (°)	100.56, 100.85, 107.78	90, 90, 90	90, 90, 90	90, 116.09, 90
Resolution range[a] (Å)	46.37–2.20 (2.28–2.20)	40.16–2.20 (2.28–2.20)	33.97–2.50 (2.59–2.50)	39.71–2.65 (2.74–2.65)
Completeness[a] (%)	97.7 (97.2)	99.8 (100.0)	99.9 (99.2)	99.3 (99.4)
R_{merge}[a] (%)	6.3 (29.8)	6.0 (44.1)	9.9 (70.4)	10.4 (56.8)
$I/\sigma I$[a]	9.3 (3.0)	14.5 (3.6)	9.4 (2.2)	5.2 (1.5)
No. of reflections				
Total[a]	195,915	101,741	308,837	57,710
Unique[a]	51,813	7,660	21,369	16,320
Refinement[b]				
R_{work}[a,c] (%)	18.7			
R_{free}[a,d] (%)	23.8			
Mean *B* value of:				
Protein (Å^2)	40.1			
Water (Å^2)	52.1			
All atoms (Å^2)	41.8			
Ramachandran plot				
Most favored region (%)	100.0			
Additional favored region (%)	0.0			
Bond RMSD[g]				
Lengths (Å)	0.003			
Angles (°)	0.635			

[a] Values in parentheses are for the highest-resolution shell.
[b] A structure was refined only for the highest-resolution crystals, belonging to space group P1.
[c] $R_{work} = (\Sigma_{hkl} ||F_{obs}| - k|F_{calc}||)/(\Sigma_{hkl}|F_{obs}|)$.
[d] R_{free} is the same as R_{work} with 5% of reflections chosen at random and omitted from refinement.
[e] The 6×His tag was not cleaved from this protein.
[f] This protein contained a point mutation, S472D, and the 6×His tag was not removed.
[g] RMSD, root mean square deviation.

mumps virus P as a template (PDB, 4EIJ; 26% identical in sequence to Nipah virus) (16, 17). AMPLE then used Molrep (28) to determine the correct positioning for one of these ensemble search models. In the successful case, the search model consisted of an ensemble of 30 structures, each a helical fragment (18 residues). This is the first successful deployment of AMPLE with comparative models deriving from a distantly homologous template.

The solution was refined with Refmac (29) and used as the starting point for a nearly complete Cα trace of the target structure using SHELXE (30). The model was brought closer to completion through the use of multiple rounds of ARP/wARP (31) and Buccaneer (32) to build side chains and missing residues. Refinement was carried out in Phenix (33), followed by manual building in Coot (34).

The asymmetric unit contains eight monomers, which have assembled into two tetrameric coiled coils. Residues 476 to 576 are visible in electron density maps for most monomers. The Nipah virus coiled coil is a few residues longer than those of the other paramyxoviruses (68 versus 56 to 64 residues) (35, 36). Analysis of potential quaternary structures with PISA suggests that these two tetramers are energetically stable, with 15,000 to 20,000 Å^2 of buried surface area and dissociation energies of 140 to 200 kcal/mol (37). The two tetramers interact at the base, burying 1,600 Å^2 in a crystal contact assembled octamer, but neither PISA nor visual inspection can identify any trimeric interaction in this crystal structure. On the basis of these findings and SEC/MALS, we posit that the Nipah virus multimerization domain forms a tetramer in solution.

The crystal structure reveals that the Nipah virus coiled coil is parallel, like that of Sendai virus and measles virus (Fig. 1A), thereby maintaining the N-terminal N^0 binding domain and the C-terminal nucleocapsid binding domains on opposite ends of the oligomeric P protein. The crystal structure of Nipah virus P also reveals that each monomer has a two-helix N-terminal cap attached at the outer top of each helix in the coiled coil. This cap structure is clearly visible in the recently reported SAXS structure (18), and it is likely that this crystal structure would fit nicely into their calculated envelope. In Sendai virus P, the cap structure is formed by three helices instead of two (15). The measles and mumps virus P proteins lack cap structures (13, 14).

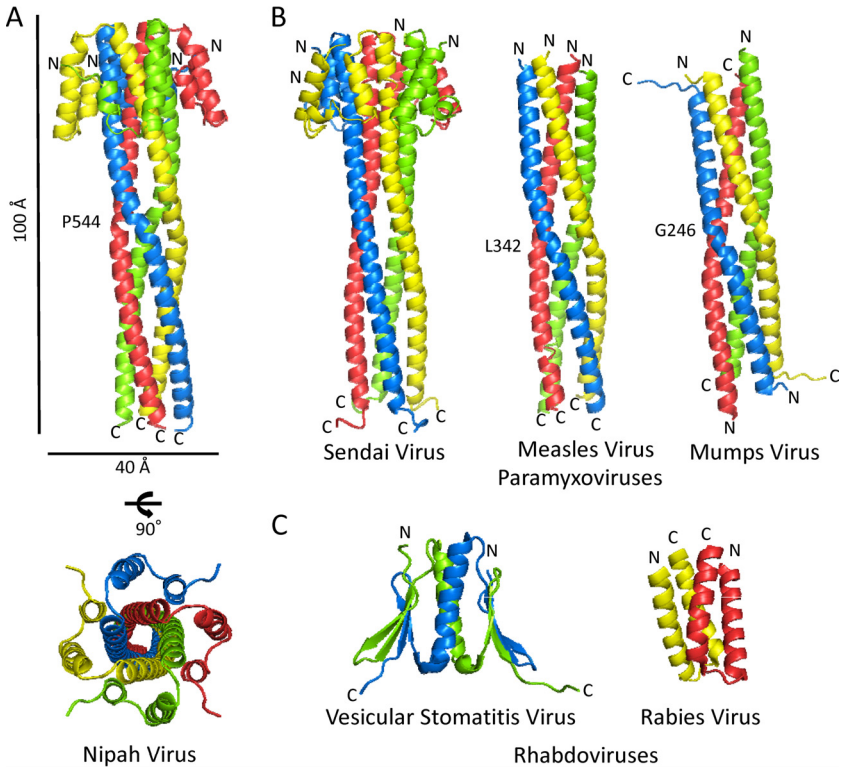

FIG 1 (A) Cartoon representations of the multimerization domain of Nipah virus P, with the dimensions, N and C termini, and residues involved in kinking indicated. (B) Cartoon representations of the multimerization domains of P from three other paramyxoviruses, Sendai virus, measles virus, and mumps virus, drawn on the same scale as Nipah virus P. Termini and residues involved in kinking of the central helices are indicated. (C) Cartoon representations of the multimerization domains of P from two rhabdoviruses, vesicular stomatitis virus and rabies virus. Both domains are dimers in solution and crystallized as dimers, but vesicular stomatitis virus has been shown to form a tetramer in the context of the RNA replication machinery (48, 49).

The Nipah virus tetramer is stabilized primarily by hydrophobic interactions typical of coiled coils (isoleucines, leucines, and valines) (38). At the N-terminal end, however, a pocket containing eight water molecules is formed by residue Gly 519, which is flanked by Ser 515 and Asn 522. These are the only water molecules found inside the channel. The measles virus and mumps virus tetramers are similarly hydrophobic, with only a few charged/polar residues and water molecules in their channels. In contrast, the interhelical channel in Sendai virus P is lined with many aromatic and polar residues and is filled with 23 water molecules and one calcium ion (15, 35). The multiple water molecules throughout the Sendai virus channel are accommodated by a larger superhelical radius (up to 9 Å wide versus 7.3 to 7.5 Å for the other viruses) and a lower superhelical frequency (twist of −1.7°/residue versus −2.8 to −3.3°/residue for the other viruses) (35). Hence, although Nipah virus and Sendai virus are the only two to have an N-terminal cap, they are assembled internally via different interactions and have different superhelical parameters. The Nipah virus structure is more typical of coiled coils, while the Sendai virus assembly is an outlier (35).

An additional difference between the Nipah virus and Sendai virus coiled coils is that the Nipah virus coiled coil contains Pro 544 in the middle of its long α-helix, which induces a kink (Fig. 1A). This kink is more reminiscent of the Leu 342-kinked measles virus and Gly 246-kinked mumps virus structures, but only in Nipah virus does this kink cause a coil frameshift, breaking from ideal Crick parameters for coiled coils (35).

It is interesting that mumps virus P gave a successful molecular replacement solution for Nipah virus P, as mumps virus P is uniquely antiparallel, while Nipah virus P, measles virus P, and Sendai virus P are all parallel (14) (Fig. 1A and B). The mumps-based model likely worked because its central kink and superhelical frequency (how twisted the oligomer is) are closer to Nipah virus than the other structures. Further, the search model did not

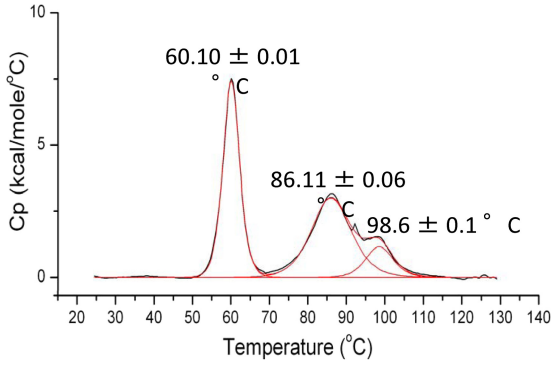

FIG 2 Thermal denaturation curve of the Nipah virus P multimerization domain collected by DSC. Normalized molar heat capacity (Cp) is plotted over a range of 25 to 130°C. The peak at 60.10°C is sharp and likely corresponds to the dissociation of the tetramer. The following two peaks at 86.11 and 98.6°C are broad and likely result from a two-state unfolding event, perhaps unfolding of the two helix cap, followed by the long helix.

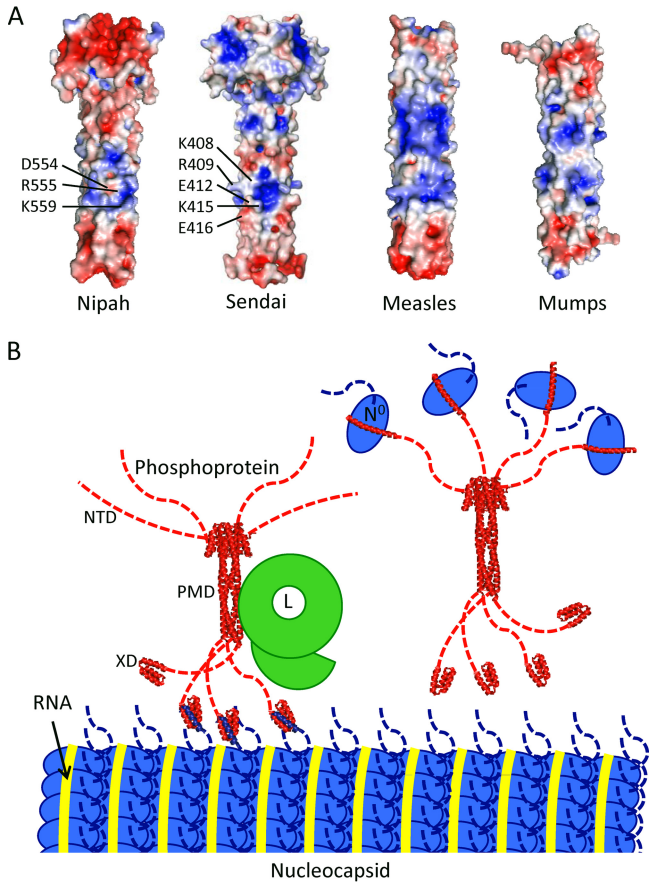

FIG 3 (A) Electrostatic surface potential representations, generated in APBS (42), of the four paramyxovirus P multimerization domain structures. The residues in a basic patch of Sendai virus P implicated in L binding are indicated (39), as are the residues in a corresponding basic patch of Nipah virus P. It is unknown if L binds this site or a different site in P, as noted for the rhabdovirus vesicular stomatitis virus (43) (B) Model of the organization of the Nipah virus replication machinery, roughly to scale, based on dimensions visualized by electron microscopy (Nipah virus nucleocapsid [44] and vesicular stomatitis virus L [44, 45]) and X-ray crystallography (this structure and the X domain of measles virus P [46]). For clarity, Nipah virus P is illustrated in either its polymerase cofactor function, in which it is bound to L and the nucleocapsid (left), or in its role as a chaperone for nascent N^0 (right). The three main domains of P (NTD, PMD, and XD) are indicated. Note that the nucleocapsid is shown in only one conformation (47) and that only about one-third of the actual width of the nucleocapsid is shown. It should also be noted that the Nipah virus L binding site has not been confirmed.

contain a cap structure (mumps virus lacks a cap, and Nipah virus and Sendai virus have differently structured caps), and the search model was a monomer, which could be placed equally well in a parallel or antiparallel fashion in molecular replacement.

Differential scanning calorimetry (DSC) suggests that the tightly coiled, hydrophobically assembled Nipah virus P multimerization domain is highly stable, undergoing transitions only at 60.1, 86.1, and 98.6°C (Fig. 2). These are likely to be the temperatures required for dissociation of the tetramer, unraveling of the helices, and unraveling of the cap structure. These data agree with the findings of Blocquel et al., who reported finding transitions at 52 and 85°C by using circular dichroism (CD) (18). The third transition point (~99°C) may not have been observed because the CD study was performed over a range of 20 to 100°C, while the DSC experiment was performed from 20 to 130°C. The central value (85°C by CD, 86°C by DSC) is comparable to the 85°C previously measured by CD for unraveling of helical secondary structure in measles virus P (13). Our DSC and SEC/MALS findings and the additional observation that the purified protein remains stably tetrameric for a year at 4°C suggest that Nipah virus P, and likely other paramyxovirus P proteins, does not easily change its oligomeric state.

In Sendai virus P, the binding site for L was found to be within the multimerization domain and several charged residues were implicated in binding (Fig. 3) (39). The corresponding residues in Nipah virus P are Asp 554, Arg 555, and Lys 559. In the Nipah virus P structure, these residues form a basic patch flanked by acidic residues. Indeed, a similar central basic patch is observed in all four paramyxovirus P structures (Fig. 3) and may function as the L binding site in each of them (39).

In conclusion, the Nipah virus P multimerization domain is a long, parallel, tetrameric, coiled coil organized with an N-terminal cap and a hydrophobic core. Although the multimerization domains of the different paramyxoviruses have low sequence identity and differ in the presence or absence of a cap and in the composition of their internal cores, all four crystal structures illustrate tetrameric coiled coils of similar lengths. The conservation and stability of this structural feature suggest that oligomerization of this type serves an essential scaffolding or organization function in the paramyxovirus life cycle. Interestingly, the multimerization domain of the P proteins of rhabdoviruses show little structural similarity to those of paramyxoviruses or to each other (Fig. 1C) (40, 41).

Protein structure accession number. The coordinates and structural factors of the Nipah virus P multimerization domain have been deposited in the Protein Data Bank under accession number 4N5B.

ACKNOWLEDGMENTS

We thank the staff of ALS Beamlines 5.02 and 4.03 and instructors of the Advanced Photon Source Data Collection Workshop and CCP4 School for assistance with data collection (Nukri Sanishvili, APS), data processing (Dominika Borek, UT Southwestern), and interpretation of Patterson maps (Andrey Lebedev, CCP4, STFC Rutherford Appleton Laboratory). We thank Kathryn Hastie and Claudia Blattner (TSRI) for help with SEC/MALS and DSC, respectively.

This work was supported by NIH training grant T32 AI00760 to the TSRI Department of Immunology and Microbial Science and by Achievement Rewards for College Scientists (J.B.J.). E.O.S. is supported by an Investigators in the Pathogenesis of Infectious Disease Award from the Burroughs Wellcome Fund.

REFERENCES

1. **Lee B, Rota PA.** 2012. Henipavirus: ecology, molecular virology, and pathogenesis. Springer, Heidelberg, Germany.
2. **Rockx B, Wang LF.** 2013. Zoonotic henipavirus transmission. J. Clin. Virol. **58:**354–356. http://dx.doi.org/10.1016/j.jcv.2013.02.013.
3. **Broder CC.** 2012. Henipavirus outbreaks to antivirals: the current status of potential therapeutics. Curr. Opin. Virol. **2:**176–187. http://dx.doi.org/10.1016/j.coviro.2012.02.016.
4. **Morin B, Kranzusch PJ, Rahmeh AA, Whelan SP.** 2013. The polymerase of negative-stranded RNA viruses. Curr. Opin. Virol. **3:**103–110. http://dx.doi.org/10.1016/j.coviro.2013.03.008.
5. **Habchi J, Longhi S.** 2012. Structural disorder within paramyxovirus nucleoproteins and phosphoproteins. Mol. Biosyst. **8:**69–81. http://dx.doi.org/10.1039/c1mb05204g.
6. **Basler CF.** 2012. Nipah and hendra virus interactions with the innate immune system. Curr. Top. Microbiol. Immunol. **359:**123–152. http://dx.doi.org/10.1007/82_2012_209.

7. **Lo MK, Peeples ME, Bellini WJ, Nichol ST, Rota PA, Spiropoulou CF.** 2012. Distinct and overlapping roles of Nipah virus P gene products in modulating the human endothelial cell antiviral response. PLoS One **7:**e47790. http://dx.doi.org/10.1371/journal.pone.0047790.
8. **Chan YP, Koh CL, Lam SK, Wang LF.** 2004. Mapping of domains responsible for nucleocapsid protein-phosphoprotein interaction of henipaviruses. J. Gen. Virol. **85:**1675–1684. http://dx.doi.org/10.1099/vir.0.19752-0.
9. **Habchi J, Blangy S, Mamelli L, Jensen MR, Blackledge M, Darbon H, Oglesbee M, Shu Y, Longhi S.** 2011. Characterization of the interactions between the nucleoprotein and the phosphoprotein of Henipavirus. J. Biol. Chem. **286:**13583–13602. http://dx.doi.org/10.1074/jbc.M111.219857.
10. **Omi-Furutani M, Yoneda M, Fujita K, Ikeda F, Kai C.** 2010. Novel phosphoprotein-interacting region in Nipah virus nucleocapsid protein and its involvement in viral replication. J. Virol. **84:**9793–9799. http://dx.doi.org/10.1128/JVI.00339-10.
11. **Chen M, Ogino T, Banerjee AK.** 2006. Mapping and functional role of the self-association domain of vesicular stomatitis virus phosphoprotein. J. Virol. **80:**9511–9518. http://dx.doi.org/10.1128/JVI.01035-06.
12. **Schneider U, Blechschmidt K, Schwemmle M, Staeheli P.** 2004. Overlap of interaction domains indicates a central role of the P protein in assembly and regulation of the Borna disease virus polymerase complex. J. Biol. Chem. **279:**55290–55296. http://dx.doi.org/10.1074/jbc.M408913200.
13. **Communie G, Crepin T, Maurin D, Jensen MR, Blackledge M, Ruigrok RW.** 2013. Structure of the tetramerization domain of measles virus phosphoprotein. J. Virol. **87:**7166–7169. http://dx.doi.org/10.1128/JVI.00487-13.
14. **Cox R, Green TJ, Purushotham S, Deivanayagam C, Bedwell GJ, Prevelige PE, Luo M.** 2013. Structural and functional characterization of the mumps virus phosphoprotein. J. Virol. **87:**7558–7568. http://dx.doi.org/10.1128/JVI.00653-13.
15. **Tarbouriech N, Curran J, Ruigrok RW, Burmeister WP.** 2000. Tetrameric coiled coil domain of Sendai virus phosphoprotein. Nat. Struct. Biol. **7:**777–781. http://dx.doi.org/10.1038/79013.
16. **Goujon M, McWilliam H, Li W, Valentin F, Squizzato S, Paern J, Lopez R.** 2010. A new bioinformatics analysis tools framework at EMBL-EBI. Nucleic Acids Res. **38:**W695–699. http://dx.doi.org/10.1093/nar/gkq313.
17. **Larkin MA, Blackshields G, Brown NP, Chenna R, McGettigan PA, McWilliam H, Valentin F, Wallace IM, Wilm A, Lopez R, Thompson JD, Gibson TJ, Higgins DG.** 2007. Clustal W and Clustal X version 2.0. Bioinformatics **23:**2947–2948. http://dx.doi.org/10.1093/bioinformatics/btm404.
18. **Blocquel D, Beltrandi M, Erales J, Barbier P, Longhi S.** 2013. Biochemical and structural studies of the oligomerization domain of the Nipah virus phosphoprotein: evidence for an elongated coiled-coil homotrimer. Virology **466:**162–172. http://dx.doi.org/10.1016/j.virol.2013.07.031.
19. **Otwinowski Z, Minor W.** 1997. Processing of X-ray diffraction data collected in oscillation mode. Methods Enzymol. **276:**307–326. http://dx.doi.org/10.1016/S0076-6879(97)76066-X.
20. **Pflugrath JW.** 1999. The finer things in X-ray diffraction data collection. Acta Crystallogr. D Biol. Crystallogr. **55:**1718–1725. http://dx.doi.org/10.1107/S090744499900935X.
21. Reference deleted.
22. **Read RJ, James MNG.** 1988. Refined crystal structure of Streptomyces griseus trypsin at 1.7 A resolution. J. Mol. Biol. **200:**523–551. http://dx.doi.org/10.1016/0022-2836(88)90541-4.
23. **Read RJ, Schierbeek AJ.** 1988. A phased translation function. J. Appl. Crystallogr. **21:**490–495. http://dx.doi.org/10.1107/S002188988800562X.
24. **Caliandro R, Dibenedetto D, Cascarano GL, Mazzone A, Nico G.** 2012. Automatic alpha-helix identification in Patterson maps. Acta Crystallogr. D Biol. Crystallogr. **68:**1–12. http://dx.doi.org/10.1107/S0108767311041353.
25. **Tu D, Li Y, Song HK, Toms AV, Gould CJ, Ficarro SB, Marto JA, Goode BL, Eck MJ.** 2011. Crystal structure of a coiled-coil domain from human ROCK I. PLoS One **6:**e18080. http://dx.doi.org/10.1371/journal.pone.0018080.
26. **Bibby J, Keegan RM, Mayans O, Winn MD, Rigden DJ.** 2012. AMPLE: a cluster-and-truncate approach to solve the crystal structures of small proteins using rapidly computed ab initio models. Acta Crystallogr. D Biol. Crystallogr. **68:**1622–1631. http://dx.doi.org/10.1107/S0907444912039194.
27. **Misura KM, Chivian D, Rohl CA, Kim DE, Baker D.** 2006. Physically realistic homology models built with ROSETTA can be more accurate than their templates. Proc. Natl. Acad. Sci. U. S. A. **103:**5361–5366.
28. **Vagin A, Teplyakov A.** 2010. Molecular replacement with MOLREP. Acta Crystallogr. D Biol. Crystallogr. **66:**22–25. http://dx.doi.org/10.1107/S0108767309045206.
29. **Murshudov GN, Skubak P, Lebedev AA, Pannu NS, Steiner RA, Nicholls RA, Winn MD, Long F, Vagin AA.** 2011. REFMAC5 for the refinement of macromolecular crystal structures. Acta Crystallogr. D Biol. Crystallogr. **67:**355–367. http://dx.doi.org/10.1107/S0907444911001314.
30. **Sheldrick GM.** 2008. A short history of SHELX. Acta Crystallogr. A **64:**112–122. http://dx.doi.org/10.1107/S0108767307043930.
31. **Langer G, Cohen SX, Lamzin VS, Perrakis A.** 2008. Automated macromolecular model building for X-ray crystallography using ARP/wARP version 7. Nat. Protoc. **3:**1171–1179. http://dx.doi.org/10.1038/nprot.2008.91.
32. **Cowtan K.** 2006. The Buccaneer software for automated model building. 1. Tracing protein chains. Acta Crystallogr. D Biol. Crystallogr. **62:**1002–1011. http://dx.doi.org/10.1107/S0907444906022116.
33. **Adams PD, Afonine PV, Bunkoczi G, Chen VB, Davis IW, Echols N, Headd JJ, Hung LW, Kapral GJ, Grosse-Kunstleve RW, McCoy AJ, Moriarty NW, Oeffner R, Read RJ, Richardson DC, Richardson JS, Terwilliger TC, Zwart PH.** 2010. PHENIX: a comprehensive Python-based system for macromolecular structure solution. Acta Crystallogr. D Biol. Crystallogr. **66:**213–221. http://dx.doi.org/10.1107/S0907444909052925.
34. **Emsley P, Lohkamp B, Scott WG, Cowtan K.** 2010. Features and development of Coot. Acta Crystallogr. D Biol. Crystallogr. **66:**486–501. http://dx.doi.org/10.1107/S0907444910007493.
35. **Grigoryan G, Degrado WF.** 2011. Probing designability via a generalized model of helical bundle geometry. J. Mol. Biol. **405:**1079–1100. http://dx.doi.org/10.1016/j.jmb.2010.08.058.
36. **Walshaw J, Woolfson DN.** 2001. Socket: a program for identifying and analysing coiled-coil motifs within protein structures. J. Mol. Biol. **307:**1427–1450. http://dx.doi.org/10.1006/jmbi.2001.4545.
37. **Krissinel E, Henrick K.** 2007. Inference of macromolecular assemblies from crystalline state. J. Mol. Biol. **372:**774–797. http://dx.doi.org/10.1016/j.jmb.2007.05.022.
38. **Ramos J, Lazaridis T.** 2011. Computational analysis of residue contributions to coiled-coil topology. Protein Sci. **20:**1845–1855. http://dx.doi.org/10.1002/pro.718.
39. **Bowman MC, Smallwood S, Moyer SA.** 1999. Dissection of individual functions of the Sendai virus phosphoprotein in transcription. J. Virol. **73:**6474–6483.
40. **Ding H, Green TJ, Lu S, Luo M.** 2006. Crystal structure of the oligomerization domain of the phosphoprotein of vesicular stomatitis virus. J. Virol. **80:**2808–2814. http://dx.doi.org/10.1128/JVI.80.6.2808-2814.2006.
41. **Ivanov I, Crepin T, Jamin M, Ruigrok RW.** 2010. Structure of the dimerization domain of the rabies virus phosphoprotein. J. Virol. **84:**3707–3710. http://dx.doi.org/10.1128/JVI.02557-09.
42. **Baker NA, Sept D, Joseph S, Holst MJ, McCammon JA.** 2001. Electrostatics of nanosystems: application to microtubules and the ribosome. Proc. Natl. Acad. Sci. U. S. A. **98:**10037–10041. http://dx.doi.org/10.1073/pnas.181342398.
43. **Takacs AM, Banerjee AK.** 1995. Efficient interaction of the vesicular stomatitis virus P protein with the L protein or the N protein in cells expressing the recombinant proteins. Virology **208:**821–826. http://dx.doi.org/10.1006/viro.1995.1219.
44. **Tan WS, Ong ST, Eshaghi M, Foo SS, Yusoff K.** 2004. Solubility, immunogenicity and physical properties of the nucleocapsid protein of Nipah virus produced in Escherichia coli. J. Med. Virol. **73:**105–112. http://dx.doi.org/10.1002/jmv.20052.
45. **Rahmeh AA, Schenk AD, Danek EI, Kranzusch PJ, Liang B, Walz T, Whelan SP.** 2010. Molecular architecture of the vesicular stomatitis virus RNA polymerase. Proc. Natl. Acad. Sci. U. S. A. **107:**20075–20080. http://dx.doi.org/10.1073/pnas.1013559107.
46. **Kingston RL, Hamel DJ, Gay LS, Dahlquist FW, Matthews BW.** 2004. Structural basis for the attachment of a paramyxoviral polymerase to its template. Proc. Natl. Acad. Sci. U. S. A. **101:**8301–8306. http://dx.doi.org/10.1073/pnas.0402690101.
47. **Egelman EH, Wu SS, Amrein M, Portner A, Murti G.** 1989. The Sendai virus nucleocapsid exists in at least four different helical states. J. Virol. **63:**2233–2243.
48. **Gao Y, Lenard J.** 1995. Cooperative binding of multimeric phosphoprotein (P) of vesicular stomatitis virus to polymerase (L) and template: pathways of assembly. J. Virol. **69:**7718–7723.
49. **Gao Y, Lenard J.** 1995. Multimerization and transcriptional activation of the phosphoprotein (P) of vesicular stomatitis virus by casein kinase-II. EMBO J. **14:**1240–1247.